Pure appl. geophys. 162 (2005) 1955–1980
0033–4553/05/101955–26
DOI 10.1007/s00024-005-2700-0

© Birkhäuser Verlag, Basel, 2005

Pure and Applied Geophysics

Observations and Numerical Simulations of Urban Heat Island and Sea Breeze Circulations over New York City

PETER P. CHILDS and SETHU RAMAN

Abstract—Observations from two SOund Detection And Ranging (SODAR) units, a 10 m micrometeorological tower and five Automated Surface Observing Stations (ASOS) were examined during several synoptic scale flow regimes over New York City after the World Trade Center disaster on September 11, 2001. An ARPS model numerical simulation was conducted to explore the complex mesoscale boundary layer structure over New York City. The numerical investigation examined the urban heat island, urban roughness effect and sea breeze structure over the New York City region. Estimated roughness lengths varied from 0.7 m with flow from the water to 4 m with flow through Manhattan. A nighttime mixed layer was observed over lower Manhattan, indicating the existence of an urban heat island. The ARPS model simulated a sea-breeze front moving through lower Manhattan during the study period consistent with the observations from the SODARs and the 10-m tower observations. Wind simulations showed a slowing and cyclonic turning of the 10-m air flow as the air moved over New York City from the ocean. Vertical profiles of simulated TKE and wind speeds showed a maximum in TKE over lower Manhattan during nighttime conditions. It appears that this TKE maximum is directly related to the influences of the urban heat island.

Key words: Urban heat island, sea breeze, TKE.

1. Introduction

Meteorological effects of urbanization are well documented throughout atmospheric literature. Most studies have focused on the urban heat island and its interactions with larger-scale atmospheric phenomena. The heat-island circulation (HIC) associated with an urban area can significantly alter lower tropospheric winds and low-level pollutant dispersion. When an urban area is located at the coast of a large body of water, complexities of the flow patterns increase because of additional circulations associated with sea and land breezes. Several studies have examined the urban heat island. SHREFFLER (1978, 1979) conducted observational studies of St. Louis, while ASAI (1970) analyzed observed data from Tokyo. Additional observational studies by TAKEUCHI and KIMURA (1976), BORNSTEIN (1975) and SAWAI (1978)

State Climate Office of North Carolina, North Carolina State University, Raleigh, NC, 27695–7236, U.S.A.

and physical modeling studies by SETHU RAMAN and ÇERMAK (1974) and MELLOR and YAMADA (1974) have focused on the urban heat island and its effects on local circulations and flow alterations. Few numerical studies have attempted to simulate the very complex micro- and mesoscale meteorology associated with urban areas such as New York City; the focus region of this study.

Atmospheric boundary layer (ABL) inhomogeneity is most apparent over a dense urban center like NYC that lies adjacent to the ocean, especially when compared to the ABL over rural, inland areas. NYC's landuse is characterized as a highly developed urban core on Manhattan Island and a sprawling dense suburban area that covers northeastern New Jersey and western Long Island. Adding to this complex urban region is a highly variable coastline consisting of many small bays, rivers and sounds (Jamaica Bay, New York Harbor, Hudson River, East River and Long Island Sound). All these features and their influence on the lower atmosphere make attempts at modeling the region difficult (MICHAEL *et al.*, 1998).

Historical studies have focused both directly and indirectly on the unique small-scale variations of the ABL in and around NYC. The NYC urban blocking effect and urban heat island phenomena have been examined in detail (BORNSTEIN and JOHNSON, 1977; BORNSTEIN *et al.*, 1994). The blocking effect can be described as the modification of the flow by an abnormally rough surface presented by Manhattan Island. The urban heat island develops because of both anthropogenic heating and heat-holding structures. This local heating further modifies the wind flow patterns over the city. Past research shows that wind speed along a streamline decreases below (increases above) those at sites outside of the city when synoptic scale winds speeds are above (below) 4 ms^{-1}. Above this critical value wind over the city is less than in rural areas and turns cyclonically as the air passes over the city due to increased frictional effect. Conversely, when the wind speed is below this value, the urban heat island tends to develop and the winds over the city are slightly stronger during both daytime and nighttime. This urban enhancement of the wind speed is a result of the increase in mesoscale baroclinicity and decrease in stability, which allows for efficient downward flux of momentum. This wind enhancement during lower wind speed regimes, especially at night, results in a more anticyclonic curvature of the wind trajectory as it passes over the city. Many studies have been performed on this topic (ANGELL *et al.*, 1971; WONG and DIRKS, 1978; LEE, 1979; DRAXLER, 1986) and most agree with this behavior of wind flow over a rough urban surface.

As a result of the urban heat island and the resulting heat island circulation, and their effect on surface-layer wind flow, numerical modeling over highly urbanized areas is complex. As the realization of potential bio-terrorism hazards in urbanized area continues to grow, reliable numerical modeling of urban areas is rapidly becoming an important research and operational issue. Studies involving high-resolution mesoscale models and pollutant dispersion models are underway (ARYA, 1999). Historically, air pollution has been regarded as a serious problem only for large cities and commercial centers. As a result of the industrial revolution and the

advent of the automobile, air quality in most of the large urban and industrialized areas has been suffering greatly. Various urban air quality models have been developed to facilitate the implementation of new strategies and techniques to help regulate pollutants being released from automobiles and industry.

The main objective of this investigation is to analyze observations and numerically simulate the mesoscale and microscale boundary layer structure over New York City. Observations from two SOund Detection And Ranging (SODAR) systems, a 10 m micrometeorological tower and five Automated Surface Observing Stations (ASOS) are examined during several synoptic scale flow regimes including the one that existed on September 11, 2001. Subsequently, a numerical simulation is conducted to explore the complex mesoscale boundary layer structure over New York City. The high resolution (1 km) numerical investigation examines the urban heat island, urban roughness effect and sea breeze structure over the region.

The National Exposure Research Laboratory, U.S. Environmental Protection Agency (EPA/NERL) has an instrumentation cluster that facilitates high-resolution temporal measurements near the surface. This ensemble consisted of three portable trailers that supported the Aerovironment Model 4000 miniSODAR, Aerovironment Model 2000 SODAR and a three-level 10 m micrometeorological tower. This cluster was deployed in lower Manhattan, New York in November 2001 to support the EPA and State Climate Office of North Carolina's study of pollutant exposure over lower Manhattan following the September 2001 disaster. To supplement these observations, data from five automated surface observation systems (ASOS) located in Newark, New Jersey, Teterboro, New Jersey, Central Park, New York, JFK Airport, New York and LaGuardia Airport, New York are also analyzed. The emphasis here is on diagnosing the synoptic scale flow regimes over the New York City during the autumn of 2001. Additionally, using the 10 m micrometeorological tower and the two SODARS, roughness length is estimated for the different flow regimes observed over the region. Observations from the ASOS and the 10 m tower are used to study the effect, if any, the urban heat island has on the temperature structure and wind fields.

A numerical simulation using the ARPS model was performed during a high ground-level pollution event observed between 13 November 2001 and 15 November 2001 over lower Manhattan (GILLIAM *et al.*, 2003). This period was characterized by light and variable winds on November 13th, with a more southwesterly component developing on the 14th and 15th. The ARPS model is used to study the effects of the urban heat island and roughness length variations on the boundary layer structure and its diurnal evolution over New York City. This simulation employs the 1 km USGS surface characteristics and 30 second terrain information to define the lower boundary. A 48-hr case study for the 1 km domain is presented. The domain is initialized from the 32-km ARPS Data Assimilation System (ADAS). A 5 km intermediate domain is utilized to ensure that accurate lateral and upper boundary conditions are ingested into the model with 1 km grid spacing. Observations from the

independent cluster and ASOS network are used to evaluate the model simulation. The 10 m tower data and the ASOS data are used to validate the model simulation of 10 m wind speed and wind direction associated with the sea breeze front and roughness induced deflections. The SODAR data are used to examine the vertical structure of the lower boundary layer and for validating the simulation of the sea breeze structure and urban heat island effect.

2. Instrumentation and Data

The miniSODAR used in this study is a high-resolution surface layer (15 to 200 m range at 5 m intervals, 10 min averaged) wind sampler. It transmits sound at a frequency of 4500 Hz, which facilitates mitigation of environmental noise interference (CRESCENTI, 1998) leading to a better representation of the surface layer wind distribution and variance. The miniSODAR has a wind speed uncertainty less than 0.50 ms^{-1} and a wind direction uncertainty of $\pm$ 5 deg. A previous study that evaluated the performance of ground-based instruments, including the miniSODAR, found a high correlation with tower measurements (CRESCENTI, 1999). SODAR systems, including the miniSODAR, use sound to sample the boundary layer emitting a pulse and receiving scatter from gradients of temperature and moisture. Turbulent mixing in the boundary layer often causes these gradients. Frequency shifts (Doppler effect) between the transmitted and returned signal are translated as moving parcels of air, and the velocity is directly related to the frequency shift. Algorithms extract other related parameters such as standard deviations of the wind components, vertical velocity, and return signal intensity (reflectivity).

The Aerovironment Model 2000 SODAR used in this study measured the same wind properties as the miniSODAR from 60 to 600 m at 30 m intervals, and averaged over a 10 min period. The Model 2000 SODAR has a wind speed error less than 0.50 ms^{-1} and a wind direction uncertainty of $\pm$ 5 deg. This unit provided important data for the convective mixed layer, and provided an independent source for comparison with the miniSODAR, while also yielding mixing height measurements below 600 m. This unit is also capable of assessing boundary layer structure and evolution after sunrise and before sunset.

The 10 m micrometeorological tower used in this study has instruments that measure wind (Young Model 05701 anemometer) at 2, 5 and 10 m along with temperature and relative humidity at 2 and 10 m. The wind direction is accurate to within $\pm$ 5 deg, while the wind speed is accurate to within 0.25 ms^{-1} at all levels. The temperature sensors are accurate to within 0.2 C at all levels. This ''ground truth'' instrumentation is important and valuable for evaluating the accuracy of the SODAR data, and provides the lower level observations that are not sampled by either SODAR. The temperature observations are also important, especially the difference between 2 m and 10 m providing valuable information regarding the static

stability of the surface layer. All tower data used in this study are sampled each second, averaged and stored at 10 min intervals. A plan view showing the location of the instrumentation cluster in lower Manhattan is shown in Figure 1.

Hourly surface observations from five National Weather Service Automated Surface Observing System (ASOS) stations are also used in this study. The stations are Newark Airport, Teterboro Airport, Central Park, LaGuardia Airport, and John F. Kennedy Airport. Quality assured hourly ASOS data were acquired from the National Climatic Data Center (NCDC) for the study period. The ASOS 10 m wind and 2 m temperature data are recorded every minute and are representative of the previous 5 min average. The data are obtained at the bottom of the hour, approximately 51 minutes past each hour. Figure 2a shows the locations of the five ASOS sites used in this study. Figure 2b shows a high-resolution photograph of lower Manhattan on 12 September 2001. The smoke plume from the World Trade Center disaster site is evident on the photograph. The instrumentation cluster was located on Pier 25 in lower Manhattan and is labeled EPA/SCO on the photograph for reference.

Figure 1
Plan view of the Lower Manhattan area, showing the location of NERL's 10 m Tower and two SODARs.

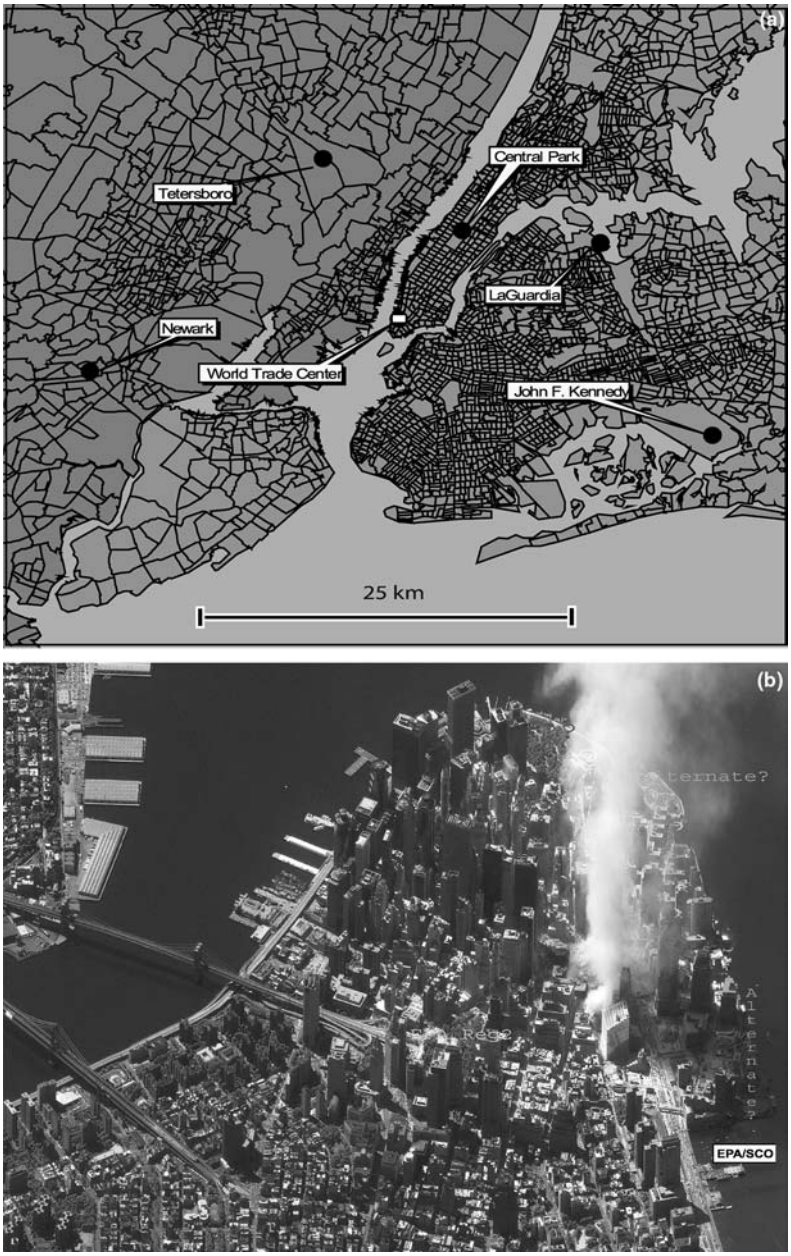

Figure 2
a A plan view of the NWS ASOS stations depicted by solid black circles and the WTC observation site, labeled at the southern tip of Manhattan Island. Figure 2b High-resolution photograph of lower Manhattan on 12 September 2001. The instrumentation cluster used in this study was located on Pier 25 (labeled EPA/SCO on the map).

3. Numerical Model

ARPS (Advanced Regional Prediction System) is a mesoscale meteorological model developed by the Center for Analysis and Prediction of Storms (CAPS), Oklahoma. ARPS was selected for this research because of its advanced physical and numerical schemes. ARPS is a non-hydrostatic, fully compressible primitive equation model suitable for simulating weather phenomena with spatial scales from several meters to several kilometers (XUE *et al.*, 1995). The ARPS uses a terrain following a vertical coordinate system with options for stretched or equal spacing while the horizontal grid spacing is equal in both the x and y directions. Prognostic variables include 3-D wind components, potential temperature, pressure, subgrid scale TKE and moisture related variables (specific humidity, cloud ice, graupel and hail).

The ARPS simulation for this study used a 1.5-order TKE turbulence closure scheme developed by SUN and CHANG (1986). In this scheme a budget equation for subgrid scale TKE is solved, which includes buoyancy, shear production, advection (diffusion and transport) and viscous dissipation. The Lin-Tao 3 Category Ice (LIN *et al.*, 1983) explicit moisture scheme is included along with the Kain Fritsch cumulus parameterization (KAIN and FRITSCH, 1993) for the water cycle in the 32 km domain. Implicit moisture physics schemes are not used in the 5 km and 1 km simulations. Radiation physics are simulated using the atmospheric radiation transfer parameterization developed at NASA/Goddard Space Flight Center, which is tailored for use in the ARPS model. This scheme includes equations for both shortwave (CHOU, 1990, 1992) and longwave (CHOU and SUAREZ, 1994) radiation processes. Details related to the above formulations are discussed in XUE *et al.* (1995, 2000, 2001). The Noilhan-Planton Land Surface Model is used to represent land surface processes over the region.

The ARPS simulation is initialized from the 32 km ARPS model analysis to generate an intermediate 5 km ARPS domain centered over New York City. For the 1 km simulation domain over New York City, the 5 km simulation domain provides initial and boundary conditions. The inner ARPS domain is shown in Figure 3. The inner domain has 50×50 grid points with 37 vertical sigma levels. The ARPS landuse data are also shown in shaded contours in Figure 3. The data are regridded to evenly fit onto the ARPS grid. Roughness length over the urban region was changed from 0.5 m to 1.5 m to account for the highly urbanized landscape associated with New York City.

4. Results and Discussion

4.1. Observational Analysis

A detailed observational analysis over the New York City area is one of the objectives of this study. The focus of this study period is 10 September 2001 through

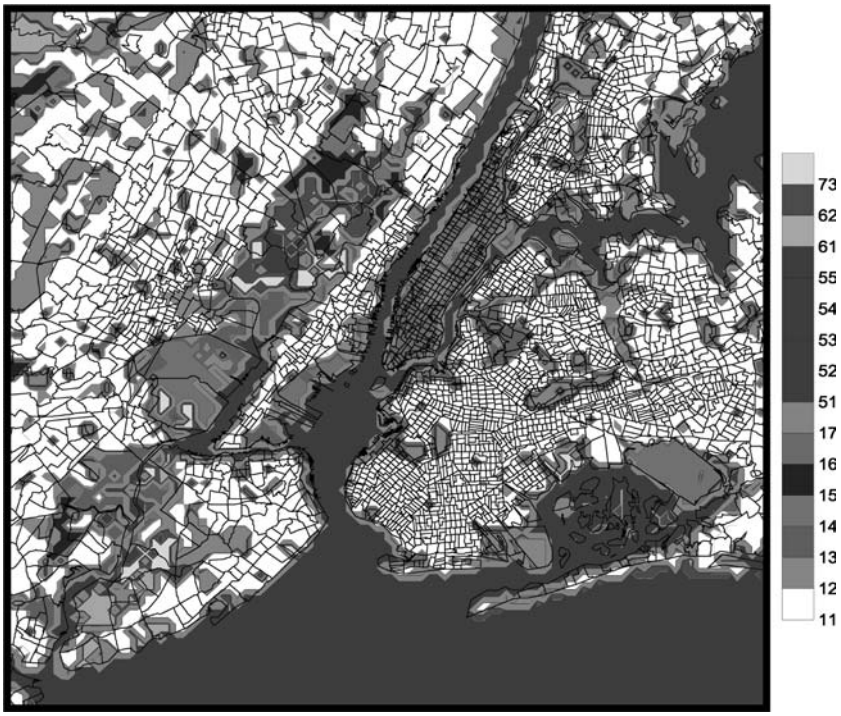

Figure 3
USGS land-use parameterization for the New York City ARPS domain. Land-use data are specified with a grid spacing of 0.9 km.

10 December 2001. Observations from five National Weather Service (NWS) ASOS sites and an independent instrumentation cluster are used in this study as described in Section 2 above.

The synoptic conditions over a three-month study period (September 11, 2001 – December 15, 2001) have been classified for each day into one of seven climatological flow regimes that normally exists during the fall season, or classified as ''other'' for different synoptic occurrences. Seasonal weather patterns affect the local meteorology and dispersion of pollutants in NYC. The mesoscale boundary layer structure and atmospheric stability vary seasonally and during different synoptic flow situations. Climatologically, a weather system passes on average every 4–6 days (BROWN and SETHU RAMAN, 1981) during the fall season. This cycle, starting after a cold front passage, typically includes a day of moderate to strong (>4–5 ms^{-1}) N-NW winds; followed by a transition day where the wind decreases as it veers from northerly to northeasterly. Next, the region experiences a day during which high pressure is centered near or directly over the area and winds become light and variable. Following this, the high pressure system moves east and winds turn southerly but remain light for a day; then as another frontal boundary approaches

from the west, southwest winds increase to moderate levels. Based on this evolution, all days during the study period have been categorized as one of these flow regimes except for a limited few that could not be grouped into the above classifications. These "other" days were mostly situations when either a strong low-pressure system impacted the area or frontal boundaries oscillated over the region, resulting in drastic wind shifts. Figure 4a shows a pie chart illustrating the synoptic flow regimes observed over the New York City region between 10 September 2001 and 10 December 2001. Seven synoptic flow regimes, along with an "other" category for complex flow patterns, are analyzed in Figure 4a. The categories are southerly, westerly and northerly with further divisions by the estimated flow strength (light or strong). The light and strong flow classification was determined by a critical wind speed of 4.0 ms^{-1} that has been linked to the urban heat island formation (BORNSTEIN and JOHNSON, 1977) and sea breeze development (ARRITT, 1993). The flow strength and direction were subjectively determined by examining six-hourly synoptic charts provided by the National Center for Environmental Prediction (NCEP) and surface observations.

The data were then classified based on a daily average of wind speed and direction. The range of wind flow for northerly regimes was defined as flow from 310° to 20°, westerly flow from 250° to 300° and southerly flow from 180° to 250°. Additionally, a light and variable and an "other" classification were included. Four flow regimes dominated: light southerly (18%), strong southerly (18%), strong westerly flow (17%), and light and variable flow (16%). These regimes occurred on 70% of the days. The remaining periods were light westerly (9%), light northerly (6%), strong northerly (7%) and other (9%), respectively. A wind rose valid 10 September 2001 through 10 December is shown in Figure 4b. Hourly observations from Newark, Central Park, LaGuardia and JFK ASOS sites valid 10 September 2001 through 10 December 2001 were used to create the wind rose. Distribution rings are labeled every 5% with wind speed ranges defined as above and below 4 ms^{-1}, as discussed above. The wind rose shows that a large percentage (35%) of wind speeds greater than 4 ms^{-1} originated from a direction between southwest and northwest. Additionally, the wind rose indicates that lighter winds were typically observed when the synoptic flow was out of the east and southeast.

4.2. Roughness Length Estimations

Large aerodynamic roughness length variations are often observed over highly urbanized terrain, such as New York City. These variations can significantly affect the surface airflow, causing a reduction in wind speed, turning of the winds, or both. The effect of the urbanized terrain on the surface winds over New York City is highly dependent on the mesoscale flow direction.

In order to quantify this effect, aerodynamic roughness lengths were estimated over lower Manhattan after separating the data into one of the four flow regimes.

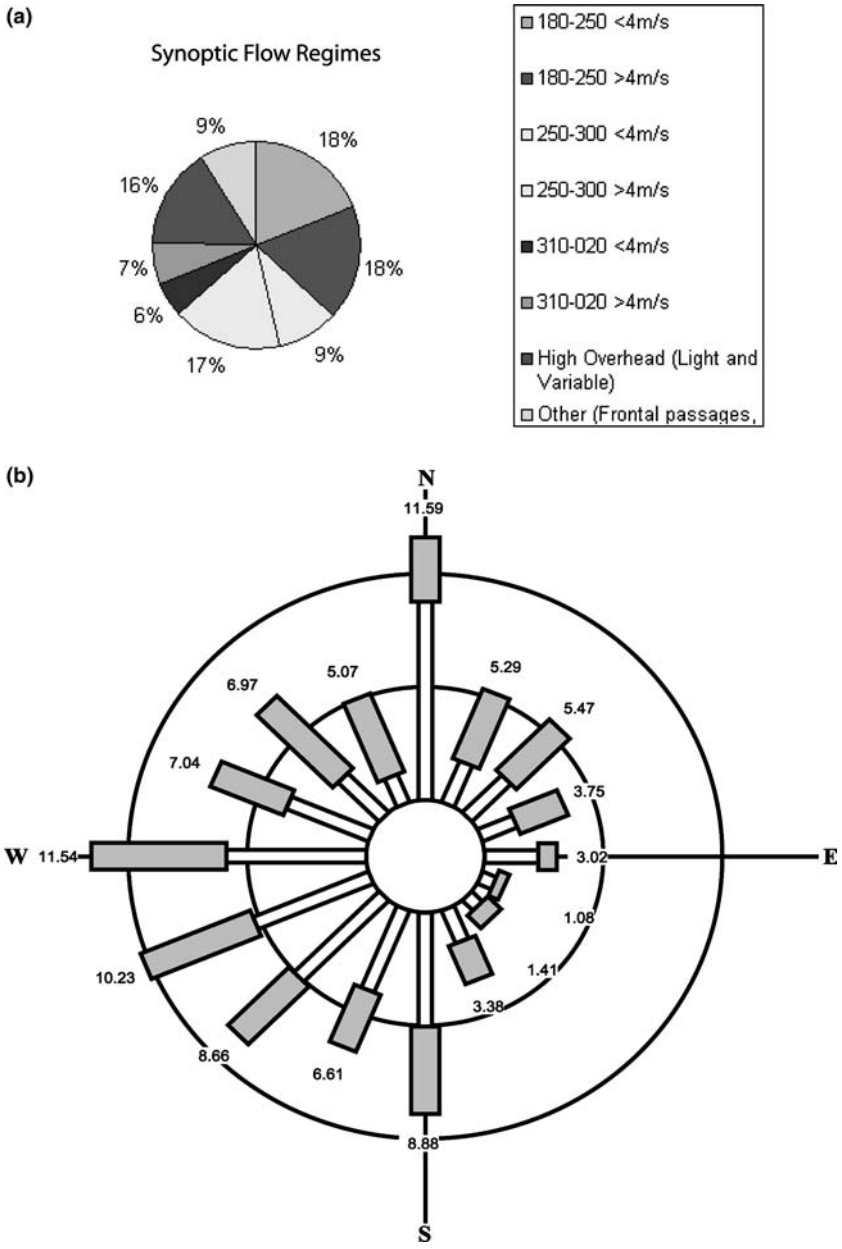

Figure 4

a Pie chart illustrating the frequencies (percentages) of the synoptic flow regimes (wind directions and speed) observed over the New York City region between 10 September 2001 and 10 December 2001. Figure 4b Wind Rose showing the distribution of wind speed and direction over the New York City area valid 10 September 2001 through 10 December 2001. Distribution rings are contoured every 5%.

These regimes include 0–89°, 90–179°, 180–269° and 270–359°. The 0–89° flow moves over the urban core of central Manhattan before reaching the WTC site, while the 90–179° flow moves over the urban core of lower Manhattan before reaching the WTC site. The 180–269° flow moves over Staten Island and the Hudson River before reaching the WTC site while the 270–359° flow moves over the Hudson River and portions of Manhattan Island before reaching the WTC site. Data from the independent 10 m tower over lower Manhattan are used to identify each flow regime. Additionally, the MiniSODAR, located in the vicinity of the 10 m tower, was used in the aerodynamic roughness length estimation. The 10 m tower and the miniSODAR became operational on 8 November 2001. The wind speed data for different flow regimes are averaged over the last month of the study period, November 10 through December 10, 2001. Wind speed and direction are averaged separately over 24-hr periods (00 UTC to 00 UTC), then classified into the appropriate flow regime based on the above conditions. Four 24-hr periods were observed for the 0–89 deg flow regime, while six 24-hr periods were classified in the 90–179 deg flow classification. Ten 24-hr periods were classified into 180–269 deg flow regime, while twelve 24-hr periods were classified into the 270–359 deg flow regime. The data were averaged over 24-hr periods to mitigate the effects of missing data from the miniSODAR.

This period was chosen because high levels of ground level pollutants, including PM-2.5, were observed over the region during this period. Monthly averaged wind speed values were calculated and then broken up into the four ranges of flow directions. The estimated aerodynamic roughness lengths for the 0–89 and 90–179 degree wind directions were approximately 3.8 m. These values seem reasonable as the flow pattern between 0 and 179 degrees is moving directly over the urban core of lower Manhattan. For the 180–269 degree flow directions, the average aerodynamic roughness length was 0.7 m, while for the 270–359 degree flow direction, the average aerodynamic roughness length was 0.9 m. Both of these lower values seem reasonable, as the flow pattern between 180 and 359 degrees moved over the Hudson River before being measured by the instrumentation cluster. Considerably lower values of aerodynamic roughness length, less than 0.01 m, are often observed over the water. However, various near-surface features, including waterfront office buildings, boat depots and even large ships and barges, influence the flow offshore in lower Manhattan. The calculated aerodynamic roughness lengths agree well with the Davenport-Wieringa roughness length classifications (STULL, 1988). This scheme classifies centers of large towns and cities, such as New York City, as chaotic with aerodynamic roughness lengths greater than 2 m.

4.3. Urban Heat Island

This section analyzes the observations during the period 00 UTC (19 LST) 13 November 2001 through 00 UTC (19 LST) 16 November 2001. High-pressure controlled the weather over much of the contiguous United States on 13 November

2001. Given the light synoptic-scale flow, local scale meteorological influences were pronounced on 13 November 2001 over the New York City region. The surface high-pressure center moved slowly off the Mid-Atlantic coast on 14 and 15 November, resulting in a light to moderate southwesterly near-surface wind flow across NYC. This period was selected to study the influences of near-surface wind flow moving off the water on the temperature and wind fields over the WTC site in lower Manhattan. Surface observations from five National Weather Service ASOS sites and a 10 m micrometeorological tower located in lower Manhattan (location of the instrumentation cluster was shown in Fig. 1) have been used in this study. Additional near-surface wind data were obtained from the Model 4000 miniSODAR located in lower Manhattan. The ASOS sites include Central Park, LaGuardia Airport, JFK Airport, Newark Airport and Teterboro (the location of the ASOS sites are shown in Fig. 2a). A surface (2 m) dry bulb temperature time series for the period 00 UTC (19 LST) 13 November 2001 through 00 UTC (19 LST) 16 November 2001 is shown in Figure 5. The daily maximum temperatures appear to be increasing throughout the study period, with an average maximum value of about 12 C observed by the stations on 13 November and a maximum value near 20 C observed on 15 November. Additionally, Central Park and LaGuardia appeared to stay warmer during the nighttime hours, as their temperatures remained nearly 2 C warmer than the other stations, including Newark, Teterboro and JFK. Observations from the 10 m micrometeorological tower in lower Manhattan were in between these extremes. The warmer temperatures observed during the nighttime in Central Park and LaGuardia were likely associated with the urban heat island, as one effect of the urban heat island is to keep surface

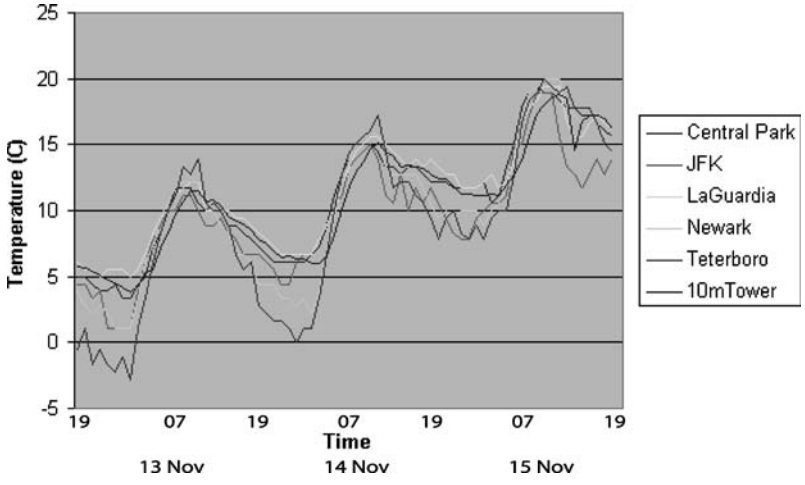

Figure 5
Surface (2 m) dry bulb temperature (c) time series valid 00 UTC (19 LST) 13 November 2001 through 00 UTC (19 LST) 16 November 2001. Five National Weather Service ASOS stations and the 10 m micrometeorological tower data are shown in color shading.

temperatures within the urban core warmer during the nighttime hours. The variability in the minimum temperature between the stations was considerably higher than the variations in maximum temperature. This may be due to light wind conditions, low mixing and differing heat capacities of the buildings and surrounding environment at the different locations. The mean temperature over the study period at Central Park and LaGuardia was between 1 and 2 C higher than the mean temperature over JFK, Newark and Teterboro, respectively. The 10 m micrometeorological tower in lower Manhattan registered a mean temperature of 10.8 C, which was less than the mean temperatures at Central Park and LaGuardia of 11.1 and 11.6 C, respectively although greater than the mean temperatures of 10.2, 9.7 and 9.2 C observed at Newark, JFK and Teterboro, respectively. Central Park, LaGuardia and the 10 m micrometeorological tower in lower Manhattan were located within the highly built-up urban core of New York City, and were likely influenced by the effects of the urban heat island which kept their temperatures warmer at night than surrounding rural locations.

A time series plot from the Model 4000 miniSODAR profile in lower Manhattan (Figure 1) for the period 12 UTC (07 LST) 13 November 2001 through 12 UTC (07 LST) 14 November 2001 is shown in Figure 6. Wind barbs are shown in standard notation. The lowest (15 m) observations are typically unreliable, therefore it should be ignored. The miniSODAR showed west to southwesterly winds at a height of 20 m between 15 UTC (10 LST) and 18 UTC (13 LST) 13 November. At approximately 19 UTC (14 LST) the 20 m winds became more southerly, and were likely associated with the passage of a sea breeze front. Another interesting feature was the vertical profile of nearly uniform wind speed and direction between 03 UTC (22 LST) 14 November and 12 UTC (07 LST) 14 November over lower Manhattan. Such a wind profile is often associated with a daytime convectively mixed boundary

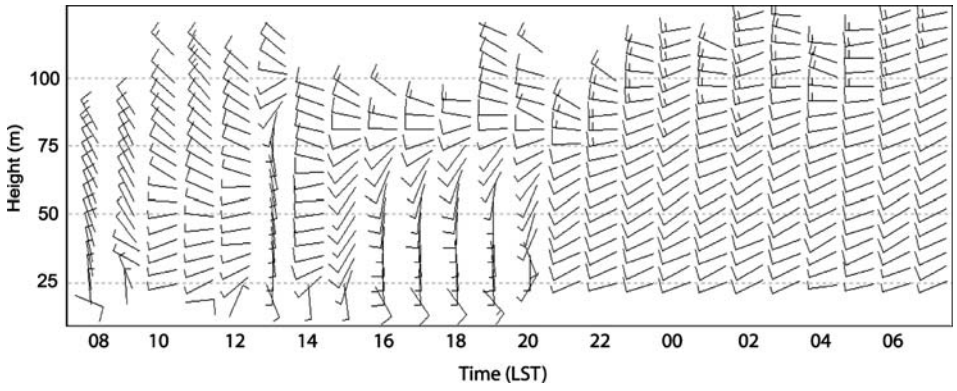

Figure 6
Model 4000-miniSODAR profile at the WTC Instrumentation site in lower Manhattan on 13–14 November 2001. Time is shown in LST.

layer. Near-surface west-southwesterly winds were advecting air into lower Manhattan that previously crossed over Staten Island. This apparent mixed layer may be the result of urban heat island induced static instability, originating over Staten Island, allowing greater turbulent mixing in the nocturnal boundary layer. However, mechanical mixing may also be contributing to this apparent mixed layer.

4.4. Numerical Simulations

Another objective of this research is to study the evolution of the mesoscale boundary layer over the New York City Metropolitan area through numerical simulations. More specifically, the urban heat island effect and sea breeze circulation will be examined in detail. Because of the highly urbanized landscape characteristics of this region, high-resolution numerical simulations are challenging. The ARPS model simulation will be compared and contrasted with surface weather observations taken during a high-pollutant concentration event over New York City in November 2001. Results from the simulation will be used to study the diurnal structure and evolution of the mesoscale boundary layer over the region.

The ARPS model was initialized at 00 UTC 13 November 2001 and integrated over a 60–hr time period until 12 UTC 15 November 2001. This period was chosen because of the formation and propagation of a sea breeze front through lower Manhattan, and also because the synoptic pattern favored the development of the urban heat island. A full synoptic review was presented as part of the Observational Analysis above. The ARPS simulation had a horizontal grid spacing of 1 km with 37 vertical sigma levels.

4.5. Simulated Surface Energy Budget

A detailed map of the New York City Metropolitan area is shown in Figure 7a. Labeled on Figure 7a are the letters B and C, which correspond to the location of surface energy budget time series, shown in Figures 7b and 7c over lower Manhattan and eastern New Jersey between 12 UTC (7 LST) 13 November and 6 UTC (01 LST) 15 November, respectively. Surface latent heat flux is shown in green, surface sensible heat flux in red and ground heat flux in black. All fluxes are plotted in W m^{-2}. There are several interesting features observed on the two time series simulations. The simulated energy budget time series over lower Manhattan, shown in Figure 7b, will be discussed first. Of interest is the occurrence of negative (downward) surface sensible heat flux between 00 UTC and 03 UTC (19 and 22 LST) on 14 November. Sensible heat flux values around negative (downward) 50 W m^{-2} were simulated during this period. By 05 UTC (00 LST), the surface sensible heat flux became positive, and remained positive (upward) until 21 UTC (16 LST). Positive surface sensible heat fluxes during the night over lower Manhattan were likely the result of the formation of urban heat island (SETHU RAMAN and ÇERMAK, 1974). The simulated energy budget time series over New Jersey is shown in Figure 7c. The

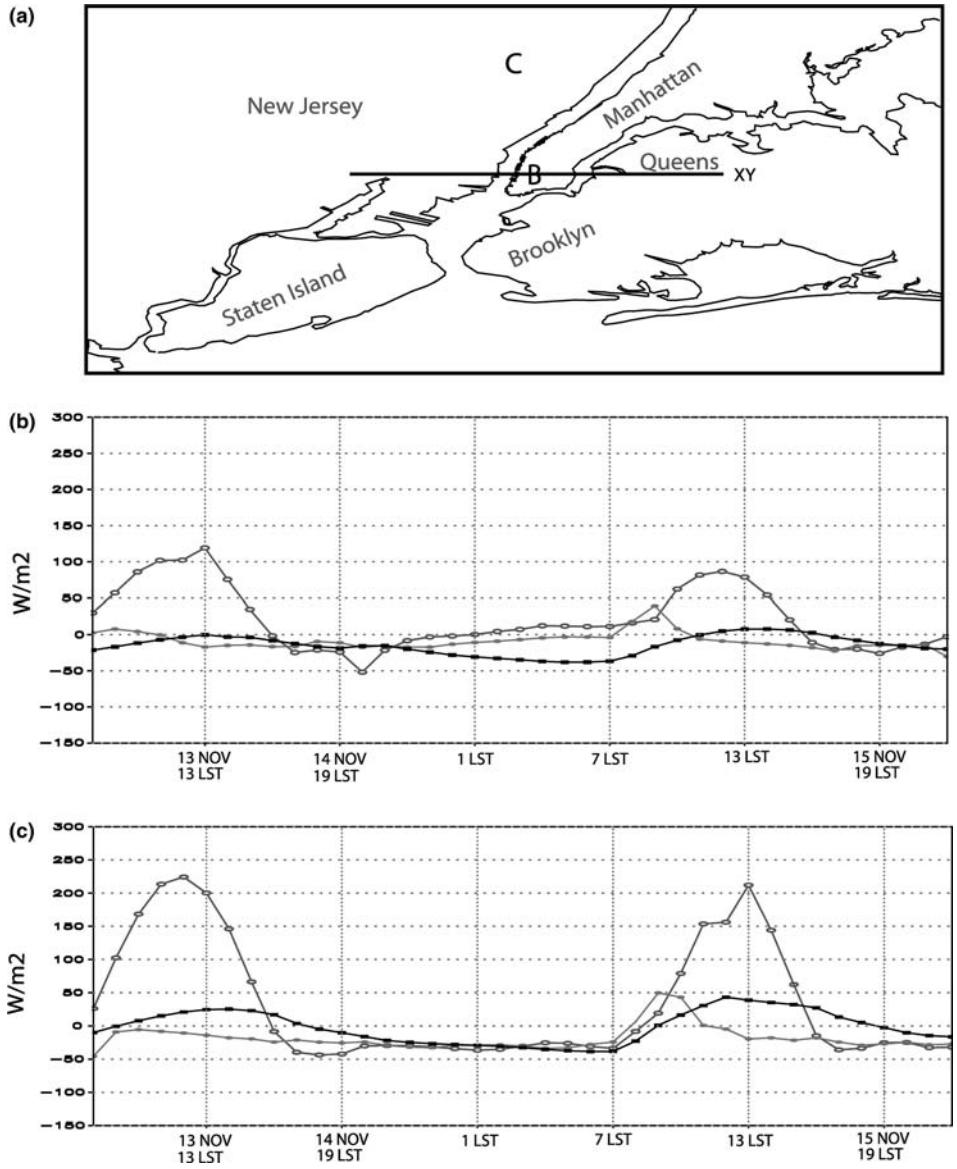

Figure 7

a Detailed map of the New York City Metropolitan area. Figures 7b and 7c show the simulated surface energy budget over lower Manhattan (labeled B on the map) and over New Jersey (labeled C on the map). Surface latent heat flux is shown in green, surface sensible heat flux is shown in red and ground diffusive heat flux is shown in black, respectively. All fluxes are simulated in W/m^{-2}.

simulated surface sensible heat flux values showed a less complex diurnal variation than the simulated surface sensible heat flux values over lower Manhattan. Over New

Jersey, the surface sensible heat flux values were positive during the daytime hours and became negative as nighttime approached (17 LST). Simulated surface sensible heat flux values remained negative throughout the night, as this region is more rural. In addition to the differences in the simulated surface sensible heat flux values during the night, the energy budget time series over lower Manhattan and New Jersey also showed differences between maximum surface sensible heat fluxes. Surface sensible heat flux values of 225 W m^{-2} were simulated over New Jersey at 17 UTC (12 LST) 13 November, while surface sensible heat flux values of 120 W m^{-2} were simulated over lower Manhattan at the same time. Additionally, surface sensible heat flux values exceeding 200 W m^{-2} were simulated over New Jersey at 18 UTC (13 LST) 14 November, while surface sensible heat flux values less than 100 W m^{-2} were simulated over lower Manhattan at the same time. The simulated surface sensible heat flux values were smaller over lower Manhattan because of the southwest flow moving over the Hudson River and Atlantic Ocean causing boundary layer airmass modification over lower Manhattan. Near-surface winds were southwesterly over New Jersey as well, however, these winds were associated with a continental airmass and did not experience any marine airmass modification. Surface latent heat flux simulations were very similar between New Jersey and lower Manhattan, close to zero. This seems reasonable, as surface latent heat flux values over a highly urbanized area are expected to be near zero, and over a residential area, slightly positive.

Several features simulated in the above surface energy budget plots exhibited the signature of an urban heat island. The surface sensible heat flux simulation time series over lower Manhattan was negative briefly during the nighttime hours of 13 and 14 November. Positive surface sensible heat fluxes are often associated with daytime conditions when incoming shortwave insolation is maximized. However, the urbanized structures associated with lower Manhattan act as heat holding materials tending to keep surface temperatures significantly warmer at night (urban heat island). In turn, positive surface sensible heat fluxes are generated over lower Manhattan, and are directly associated with the effects of the urban heat island.

4.6. Simulated Sea Breeze Structure

Wind velocity vectors and vertical velocity (contoured in ms^{-1}) at 100 m above the surface valid 15 UTC (10 LST) 13 November are shown in Figure 8a. The 100 m wind flow generated winds out of the north over much of the domain, becoming more westerly over and just to the east of Staten Island. Observing the vertical velocity contours, an enhancement in upward vertical motion was simulated over and just east of Staten Island where upward vertical velocities were near 0.15 ms^{-1}. To the north of this boundary winds were moving from the north and northeast, while to the south of the boundary, winds were moving from the south and southwest. The independent 10 m tower over lower Manhattan, shown in plan view in Figure 1, validated the model simulation, showing south-southwesterly winds associated with

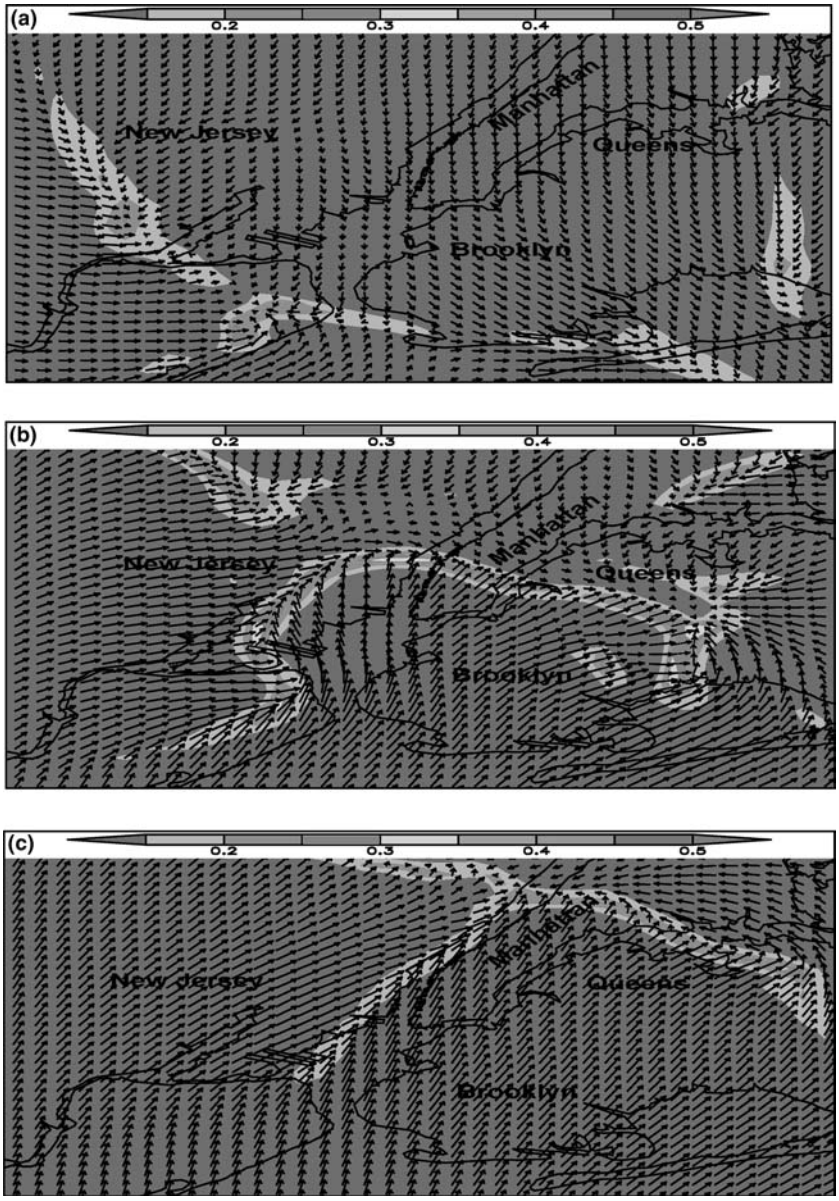

Figure 8

ARPS simulated 100 m wind velocity vectors (m/s) and vertical velocity contours (shown in grayscale defined by the overhead color bar) in m/s. Figure 8a is valid 15 UTC (10 LST) 13 November 2001. Figure 8b is valid 18 UTC (13 LST) 13 November 2001. Figure 8c is valid 21 UTC (16 LST) 13 November 2001.

the passage of the sea breeze front. Observed surface temperatures over land were 12C, while sea-surface temperatures (SST) were observed near 8C. This thermal gradient was strong enough to develop a sea breeze front over the region.

Another interesting feature is the area of enhanced wind speeds simulated over New York Harbor. The ARPS simulation was initialized with the Advanced Very High Resolution Radiometer (AVHRR) SST analyses archived at 1.44 km to allow for a more accurate simulation of boundary layer features along the land-water interface. Figure 8b delineates 100 m wind velocity vectors and vertical velocity (multi-color contoured in ms^{-1}) valid 18 UTC (13 LST) 13 November. A very distinct convergence boundary was observed over the region as an omega-like pattern. The convergence boundary stretched from Staten Island northward into New Jersey, and then spread eastward across lower Manhattan into Queens and Brooklyn before turning southward into Jamaica Bay. Associated with this convergence zone are areas of enhanced upward vertical velocities. Model simulated upward vertical velocities are between 0.2 and 0.35 ms^{-1} as seen in Figure 8b. BORNSTEIN *et al.* (1994) performed numerical simulations over the same area and observed a similar frontal alignment that extended through Staten Island, across lower Manhattan and eastward through Queens and Brooklyn. Figure 8c shows 100 m wind velocity vectors and vertical velocity (contoured in ms^{-1}) valid 21 UTC (16 LST) 13 November. A region of enhanced convergence and vertical motion is simulated over northern Manhattan. This is likely associated with the northernmost extent of the sea breeze's inland propagation. Upward vertical velocity values exceeding 0.2 ms^{-1} were simulated as a result of the low-level convergent forcing.

Figure 9 depicts a model simulated vertical cross section extending from west to east across the NYC Metropolitan area shown as XY in Figure 7a. Wind barbs (ms^{-1}) and vertical velocity (ms^{-1}) are shown as shading for this cross section in Figure 9. Two regions of enhanced upward vertical motion are simulated. The first region is over New Jersey, where a maximum upward vertical velocity of 0.7 ms^{-1} is simulated. This matched the area of enhanced 100 m level convergence simulated over the same region shown in Figure 8b. Another region of enhanced upward vertical motion is evident over Queens and Brooklyn. A well-defined maximum upward vertical motion exceeding 0.6 ms^{-1} was simulated over this region, agreeing closely with the zone of enhanced 100 m convergence simulated in Figure 8b over the same area. With southerly winds simulated in the lowest 250 m of the vertical cross section and westerly to northwesterly winds simulated above 300 m, this frontal feature is shallow in its vertical extent. This simulated feature agrees well with previous research by MICHAEL *et al.* (1998) and BORNSTEIN *et al.* (1994), which showed similar results using Weather Surveillance Radar 88 Doppler (WSR-88D) imagery and numerical simulations, respectively.

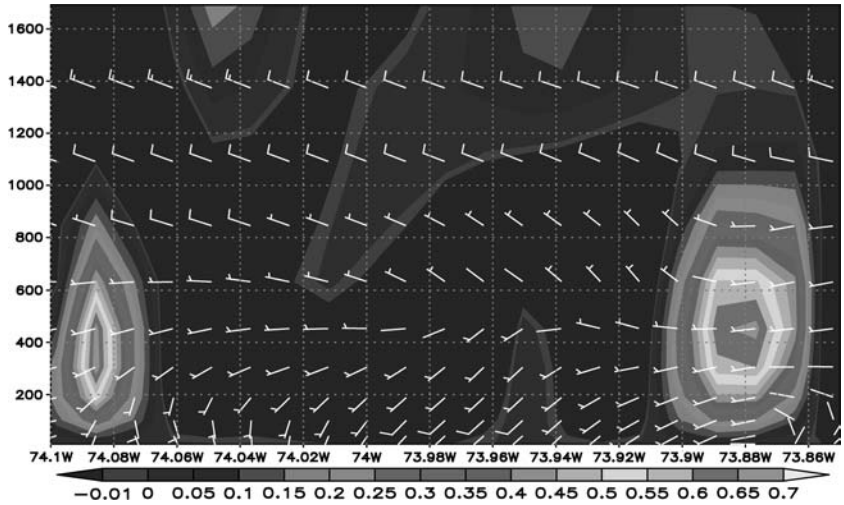

Figure 9
Vertical Velocity (m/s) cross section (m) through a sea-breeze front over extreme southern Manhattan Island valid 18 UTC (13 LST) 13 November 2001.

4.7. Urban Heat Island

Model estimated 10 m wind direction (vectors), and speed (contoured in ms^{-1}), at 03 UTC (22 LST) 14 November is shown in Figure 10a. Surface wind observations (ms^{-1}) are shown in red. A very complex wind flow pattern is shown in Figure 10a. Southwesterly winds in excess of 4 ms^{-1} were simulated over New York Harbor. As the winds entered the urban core of lower Manhattan they began to slow to less than 2 ms^{-1} and back cyclonically, becoming more southerly over central Manhattan Island. A region of calm winds with speeds less than 0.5 ms^{-1} was simulated over Brooklyn and extreme eastern lower Manhattan. This calm wind was likely a result of the frictional drag caused by the high roughness length associated with lower Manhattan and Brooklyn. Model estimated 100 m wind direction (vectors) and speed (contoured in ms^{-1}) at 03 UTC (22 LST) are shown in Figure 10b. Similar to the 10 m winds, the 100 m winds slowed from 10 ms^{-1} to 6 ms^{-1} as they moved over the more urbanized landscape associated with Manhattan and Brooklyn. However, unlike the 10 m winds, the 100 m winds did not turn cyclonically, remaining southwesterly throughout the entire region. Variations in building height and drag likely resulted in the shallow nature of this cyclonic turning. This feature agrees with observational findings by BORNSTEIN and JOHNSON (1977) that showed nighttime events during stronger flow regimes (>4 ms^{-1}) were associated with distinctive roughness induced cyclonic turning in the winds over the main core of Manhattan and Brooklyn.

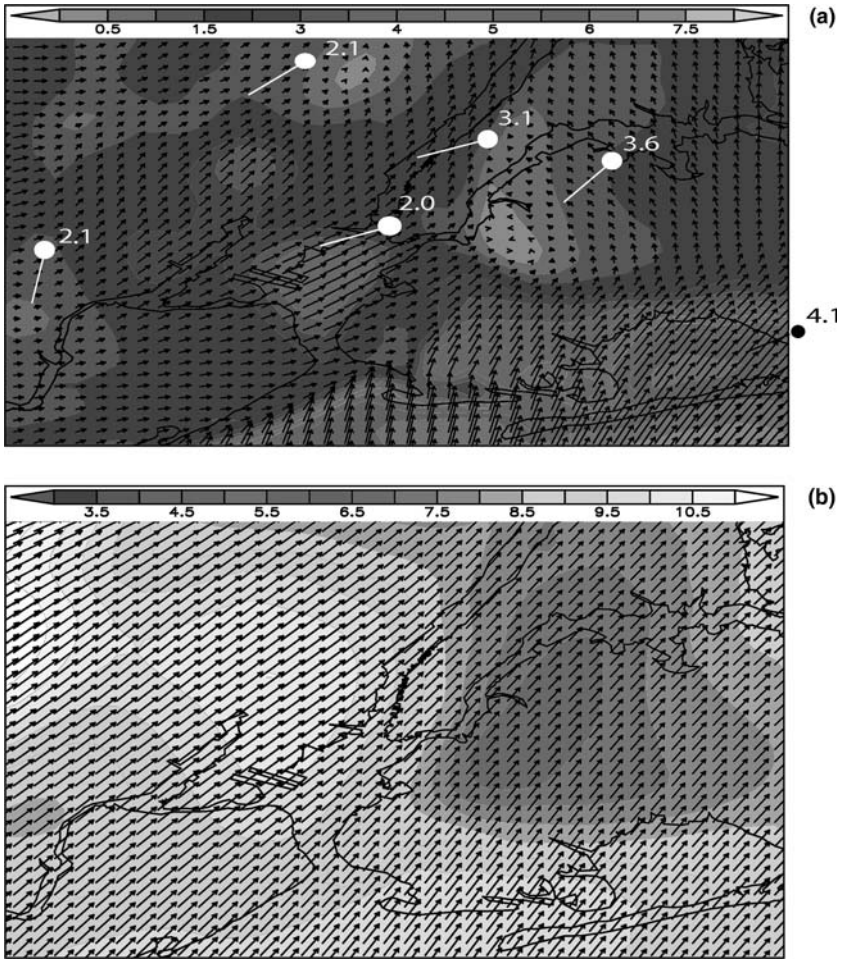

Figure 10
a ARPS simulated 10 m wind velocity (m/s) valid 03 UTC (22 LST) 14 November 2001. 10 m wind observations shown in white with the barb showing wind direction from, and number indicating speed (m/s) Figure 10b ARPS simulated 100 m wind velocity (m/s) valid 03 UTC (22 LST) 14 November 2001.

Vertical TKE ($m^2\ s^{-2}$), wind speed (kts, 1 kt = 0.52 ms^{-1}) and potential temperature (K) time series over the World Trade Center (WTC) disaster recovery site valid 12 UTC (7 LST) 13 November through 6 UTC (01 LST) 15 November is shown in Figure 11. A SODAR profile observed at the WTC Instrumentation Site in lower Manhattan from 12 UTC 13 November through 12 UTC (07 LST) 14 November (time is shown in both local and UTC formats) was shown in Figure 6. Wind barbs are shown using the standard notation. From Figure 11, several features are apparent. The first feature analyzed is the region of maximum TKE simulated

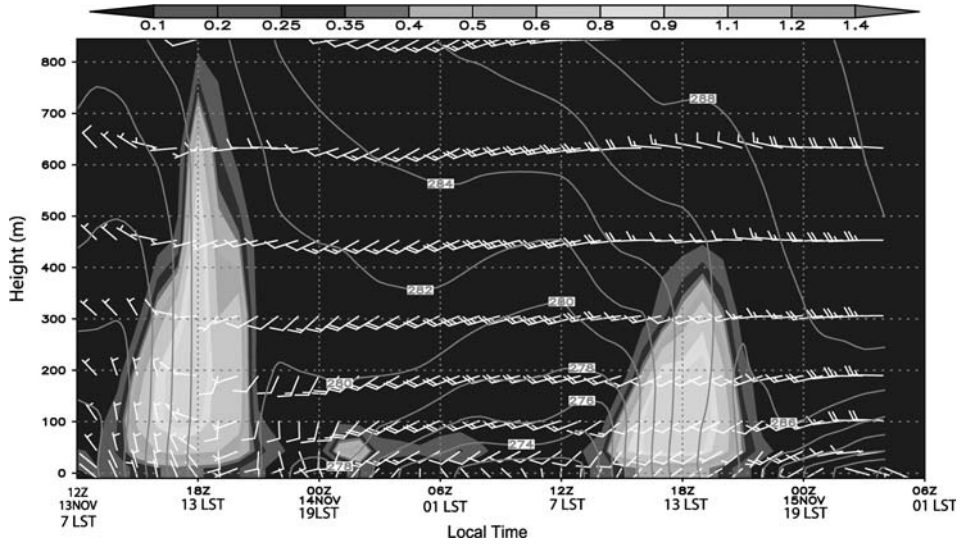

Figure 11
Time series vertical profile of turbulent kinetic energy (m^2/s^2), horizontal wind (kt) and potential temperature (K) simulated by ARPS at the WTC site. TKE is shaded, potential temperature is contoured and wind is shown by standard barbs notation in knots.

between 16 UTC (11 LST) and 19 UTC (14 LST) 13 November. Boundary layer heights reached nearly 800 m at 18 UTC (13 LST), with TKE values greater than 1.2 $m^2\ s^{-2}$ between the altitudes of 300 m and 450 m. Another feature is the boundary layer wind field between 16 UTC and 19 UTC (11 LST and 14 LST). Winds below 300 m were simulated from the north with a magnitude of 5 kts ($\sim$ 3 ms^{-1}). Between 18 and 19 UTC (13 and 14 LST), the wind direction changed from northerly to southerly following the passage of the sea breeze front. Data from the SODAR, shown in Figure 6, verifies the ARPS simulation, showing the wind shift from northerly to southerly around 18 UTC (13 LST). Additionally, there is a region of enhanced turbulence and wind speed simulated for the time period between 01 and 08 UTC (20 and 03 LST) 14 November with low-level winds simulated between 10 and 15 kts (5 to 8 ms^{-1}). Analysis from the SODAR data also revealed a region of maximum low-level winds of 15 kts (8 ms^{-1}) observed at 00 UTC (19 LST) 14 November. This feature may be a result of the low-level convergence associated with the urban heat island effect and will be more thoroughly discussed below. After 02 UTC (21 LST) 14 November, the low-level wind flow was simulated and was also observed out of the southwest at 10 kts (5 ms^{-1}). Another region of maximum TKE and boundary layer height was simulated between 16 UTC and 21 UTC (11 and 16 LST) 14 November. This regime differed significantly from the boundary layer structure on 13 November. For example, the maximum boundary layer height was

approximately 400 m lower on 14 November than it was on 13 November (800 m). The maximum TKE simulated on 14 November was less than 0.95 m^2 s^{-2}, which was observed at 18 UTC (13 LST). This was significantly less than the 1. 2 m^2 s^{-2} of TKE simulated on 13 November. The decrease in simulated TKE was likely the result of increased static stability seen in the potential temperature distribution. It is apparent from examining the time series and SODAR data that the synoptic scale wind flow overwhelmed any mesoscale and microscale meteorological processes directly related with the urban heat island after 08 UTC (03 LST) 14 November. Southwesterly winds of 10 kts (5 ms^{-1}) and greater were observed during this time period, keeping the boundary layer well mixed and homogeneous over the study area.

Figure 12 presents a model simulated vertical cross section of TKE, displayed from west to east along the line XY shown in Figure 7a. The cross section was centered over the World Trade Center disaster recovery site (40.50°N–74°W). Shown in Figure 12 are wind barbs and TKE (m^2 s^{-2}) valid 18 UTC (13 LST) 13 November, just as the sea breeze front was moving into lower Manhattan. A localized TKE maximum exceeding 1.1 m^2 s^{-2} was simulated over New Jersey, the boundary layer height decreased from 600 m at 17 UTC (12 LST) 13 November, to less than 550 m at 18 UTC (13 LST). The model also simulated a relative minimum of turbulent energy between New Jersey and Manhattan over water. This air column, directly over the Hudson River, registered TKE readings near 0.7 m^2 s^{-2}, and was likely associated with a more stable maritime airmass. A maximum in TKE, exceeding

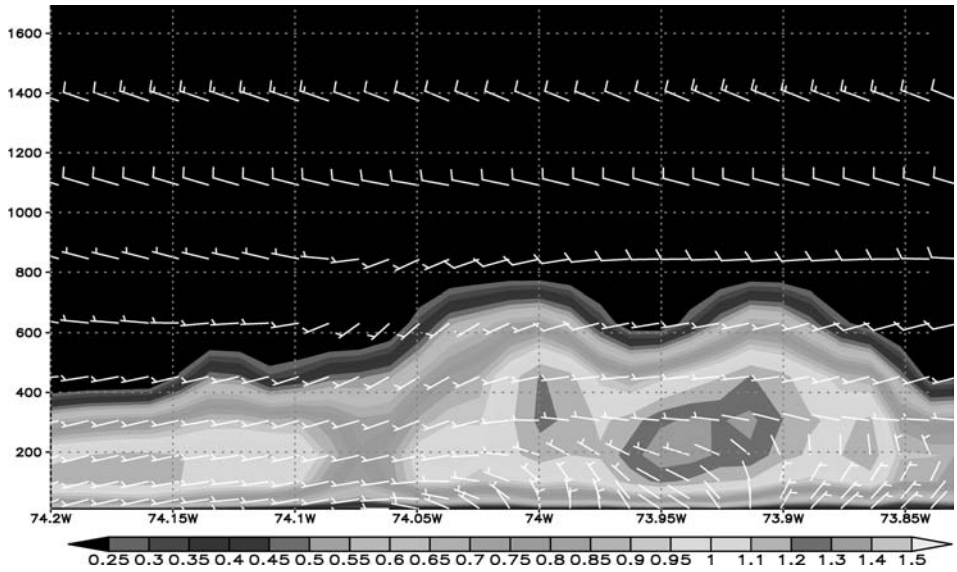

Figure 12
Vertical cross section (m) of TKE (m^2/s^2) and wind barbs valid at 40.50 N at 18 UTC (13 LST) 13 November 2001.

1.2 $m^2 s^{-2}$, was evident directly over lower Manhattan. The boundary layer height was also maximized in this region, approaching 800 m, experiencing a growth of nearly 400 m between 17 UTC and 18 UTC (12 and 13 LST). This rapid growth was likely associated with greater amounts of surface layer heating which was a direct result of the largely urbanized land use. To the east of this feature was a localized minimum in boundary layer height, approximately 600 m, associated with the more statically stable East River. Boundary layer heights quickly rebounded east of this region, over Long Island, and again approached 800 m. TKE is also maximized over Long Island, with values exceeding 1.3 $m^2 s^{-2}$. The TKE maximum was located at a depth of 200 to 300 m, or approximately one-third the height of the boundary layer, which agreed with the expected region of maximum turbulent energy (STULL, 1988). The wind flow was generally from the north over the lowest 100 m of the simulated cross section, with the exception of a more westerly component developing over New Jersey. This component is a result of the developing convergence zone associated with the strengthening sea breeze front south of lower Manhattan. Above 100 m, 5 ms^{-1} westerly winds are simulated over New Jersey and Manhattan, while a northwesterly wind associated with enhanced turbulent energy was simulated above 100 m over western Long Island. Over eastern Long Island the wind field above 100 m was out of the north and northeast at 5 ms^{-1}.

5. Summary and Conclusions

Observations from several instrumentation platforms were examined during different synoptic scale flow regimes over NYC. A numerical simulation was conducted to explore the urban heat island, urban roughness effect and sea breeze structure over the NYC region.

Additionally, the effects of wind directions on the roughness lengths observed over lower Manhattan were also analyzed. The roughness lengths varied from 0.7 m with a westerly flow over water to about 4 m with a flow through Manhattan. A nighttime mixed layer was observed over lower Manhattan This apparent mixed layer may be the result of urban heat island induced static instability, originating over Staten Island, allowing greater turbulent mixing in the nocturnal boundary layer.

Simulated surface energy budget also shows the presence of an urban heat island. The ARPS model simulated the development and inland penetration of the sea breeze front over the region. The sea breeze front formed because of strong differential heating between the land of the region and the Atlantic Ocean, in the presence of a light and variable synoptic scale flow. The mesoscale model simulated the sea breeze front moving through lower Manhattan during this period and agreed well with both SODAR and 10 m tower observations from an independent instrumentation cluster maintained by the EPA and State Climate

Office of North Carolina in lower Manhattan. The general structure of the sea breeze front over the region also agreed with previous studies by BORNSTEIN, *et al.* (1994), who performed numerical simulations over the same area and observed a similar frontal alignment that extended through Staten Island, across lower Manhattan and eastward through Queens and Brooklyn.

The nocturnal boundary layer was also studied using surface and 100 m wind simulations, as well as surface energy budget figures and TKE cross sections. Wind simulations revealed a slowing and cyclonic turning of the 10 m wind as the flow moved over Brooklyn, Queens and Manhattan, while 100 m wind simulations reflected a slowing of the wind flow, however no discernable alteration of flow directions. This simulated feature is in agreement with observational findings by BORNSTEIN and JOHNSON (1977) that showed nighttime events during stronger flow regimes (>4 ms^{-1}) were associated with distinctive roughness-induced cyclonic turning in the winds over the main core of Manhattan and Brooklyn.

Vertical profiles of TKE and wind velocity were also examined. Several simulated profiles showed a maximum in TKE over lower Manhattan during nighttime conditions. It appears that this TKE maximum is directly related to the influences of the urban heat island. The simulated location and structure of the nocturnal boundary layer over lower Manhattan are consistent with the results and agreed well with previous research on urban heat islands by SETHU RAMAN and ÇERMAK (1974) and BORNSTEIN and JOHNSON (1977).

Additional near-surface wind and temperature data are needed to further evaluate the numerical model's ability to accurately simulate the mesoscale boundary layer over NYC. These data could also be used for data assimilation into the numerical models.

Acknowledgements

This work was supported by the State Climate Office (SCO) of North Carolina and the U.S. Environmental Protection Agency (U.S. E.P.A.). The SODAR observations were made as part of a joint project with the U.S. E.P.A. The authors thank Dr. Alan Huber (U.S. E.P.A.) for several helpful discussions and also in obtaining the data. Ryan Boyles, Robert Gilliam, and Ameenulla Syed of the SCO also assisted in obtaining the observations. The authors thank Ryan Boyles for technical assistance in preparing this manuscript.

REFERENCES

ANGELL, J.K., PACK, D.H., DICKSON, C.R., and HOECKER, W.H. (1971), '*Urban Influence on Nighttime Airflow Estimated from Tetroon Flights*', J. Appl. Meteor. *10*, 194–205.

ARRITT, R.W. (1993), *Effects of Large-scale Flow on Characteristic Features of the Sea Breeze*, J. Appl. Meteor. *32*, 116–125.

ARYA, S.P., *Air Pollution and Dispersion Meteorology* (Oxford University Press, New York 1999).

ASAI, T. (1970), *Thermal Instability of a Plane Parallel Flow with Variable Vertical Shear and Unstable Stratification,* J. Meteor. Soc. Japan *48*, 129–139.

BORNSTEIN R.D., THUNIS, P., and SCHAYES, G., *Observation and Simulation of Urban-topography Barrier Effects on Boundary Layer Structure Using the Three-dimensional TVM/URBMET Model. "Air Pollution and its Application X"* (Plenum Press, New York 1994).

BORNSTEIN R.D. and JOHNSON, D.S. (1977), *Urban-rural Wind Velocity Difference*, Atmos. Environ *11*, 597–604.

BORNSTEIN R.D. (1975), *The Two-dimensional URBMET Urban Boundary Layer Model*, J. Appl. Meteor *14*, 1459–1477.

BROWN, R.M. and SETHURAMAN, S. (1981), *Temporal Variation of Particle Scattering Coefficients at Brookhaven National Laboratory, New York*, Atmos. Environ. *15*, 1733–1737.

CHOU, M.-D. (1990), *Parameterization for the Absorption of Solar Radiation by O_2 and CO_2 with Application to Climate Studies,* J. Climate *3*, 209–217.

CHOU, M.-D. (1992), *A Solar Radiation Model for Climate Studies,* J. Atmos. Sci. *49*, 762–772.

CHOU, M.-D. and SUAREZ, M.J. (1994), *An Efficient Thermal Infrared Radiation Parameterization for Use in General Circulation Models,* NASA Tech. Memo. 104606, 85 pp.

CRESCENTI, G.H. (1998), *The Degradation of Doppler SODAR Performance due to Noise: A Review,* Atmos. Environ. *32*, 1499–1509.

CRESCENTI, G.H. (1999), *A Study to Characterize Performance of Various Ground-based Remote Sensors,* NOAA Technical Memorandum ERL ARL-229, 286 pp.

DRAXLER, R.R. (1986), *Simulated and Observed Influence of the Nocturnal Urban Heat Island on the Local Wind Field,* J. Climate Appl. Meteor. *25*, 1125.

GILLIAM, R.G., CHILDS, P.P., HUBER, H., and RAMAN, S. (2003), *Metropolitan Scale Transport and Dispersion from the New York World Trade Center Following September 11, 2001. Part I: An Evaluation of The CALMET Meteorological Model,* NOAA Technical Memorandum.

GILLIAM, R.G. (2001), *Influence of Surface Heterogeneities on the Boundary Layer Structure and Diffusion of Pollutants,* M.S. Thesis, Department of Marine, Earth and Atmospheric Sciences. N.C. State University, Raleigh, NC.

KAIN, J.S. and FRITSCH, J.M. (1993), *Convective parameterization for mesoscale models: The KAIN-FRITSCH* scheme. In: *The Representation of Cumulus Convection in Numerical Models, Meteor. Monogr.*, Amer. Meteor. Soc. 165–170.

LEE, D.O. (1979), *The Influence of Atmospheric Stability and the Urban Heat Island on Urban-rural Wind Speed Differences.* Atmos. Environ. *13*, 1175–1180.

LIN, Y.-L., FARLEY, R.D., ORVILLE, H.D. (1983), *Bulk Parameterization of the Snow Field in a Cloud Model,* J. Climate Appl. Meteor. *22*, 1065–1092.

MELLOR, G.L. and YAMADA, T. (1974), *A Hierarchy of Turbulence Closure Models for Planetary Boundary Layers,* J. Atmos. Sci. *31*, 1791–1806.

MICHEAL, P., MILLER, M., and TONGUE, J.S. (1998), *Sea breeze regimes in New York City region—Modeling and Radar Observations,* Transact. Second Conf. Coastal Atmospheric and Oceanic Prediction and Processes, 78th AMS Annual Meeting, 11–16 January 1998, Phoenix, Arizona.

SAWAI, T. (1978), *Formation of the Urban Air Mass and the Associated Local Circulations*, J. Meteor. Soc. Japan. *56*, 159–173.

SETHU RAMAN, S. and CERMAK, J.E. (1974), *Physical Modeling of Flow and Diffusion over an Urban Heat Island,* Adv. in Geophys. *18B*, 223–240.

SHREFFLER, J.H. (1978), *Detection of Centripetal Heat Island Circulations from Tower Data in St. Louis,* Bound.-Layer Meteor. *15*, 229–242.

SHREFFLER, J.H. (1979), *Heat Island Convergence in St. Louis during Calm Periods,* J. Appl. Meteor. *18*, 1512–1520.

STULL, Roland B, *An Introduction to Boundary Layer Meteorology* (Kluwer Academic Publishers, Norwell, MA 1988).

Sun, W.Y. and Chang, C.Z. (1986), *Diffusion Model for a Convective Layer. Part I: Numerical Simulation of Convective Boundary Layer*. J. Climate Appl. Meteor. *25*, 1445–1453.

Takeuchi, K. and Kimura, F. (1976), *Numerical Simulation of Photochemical Smog in Tokyo Metropolitan Area,* Pap. Meteor. Geophys. *27*, 41–53.

United States Geological Survey, Land Use Land Cover Data (LULC), Web address: http://edc.usgs.gov/products/landcover/lulc.html

Wong, K.K. and Dirks, R.A. (1978), *Mesoscale Perturbations on Airflow in the Urban Mixed Layer*. J. Appl. Meteor. *17*, 677–688.

Xue, M., Droegemeier, K.K., and Wong, V. (1995), *Advanced Regional Prediction System (ARPS) and Real-time Storm Prediction,* Preprint, International Workshop on Limited-area and Variable Resolution Models, Beijing, China, World Meteor. Organ.

Xue, M., Droegemeier, K.K., and Wong, V. (2000), *The Advanced Regional Prediction System (ARPS)-A Multi-scale Nonhydrostatic Atmospheric Simulation and Prediction Tool. Part I: Model Dynamics and Verification*, Meteor. Atmos. Phys. *75*, 161–193.

Xue, M., Droegemeier, K.K., Wong, V., Shapiro, A., Brewster, K., Carr, F., Weber, D., Liu, Y., and Wang, D. (2001), *The Advanced Regional Prediction System (ARPS) – A Multi-scale Nonhydrostatic Atmospheric Simulation and Prediction Tool. Part II: Model Physics and Applications,* Meteor. Atmos. Phys. *76*, 143–165.

(Received May 3, 2004, accepted October 20, 2004)
Published Online First: June 21, 2005


To access this journal online:
http://www.birkhauser.ch